J Mater Sci: Mater Med (2017) 28:54
DOI 10.1007/s10856-017-5864-0

Original Research

Safety and efficacy of a novel abluminal groove-filled biodegradable polymer sirolimus-eluting stent

Jinzhou Zhu[1] · Huizhu Liu[1] · Haipo Cui[2] · Zhirong Tang[2] · Chengli Song[2] · Ruiyan Zhang[1]

Received: 2 January 2017 / Accepted: 30 January 2017 / Published online: 14 February 2017

Abstract Late stent thrombosis (LST) following drug-eluting stent (DES) implantation in patients with coronary artery disease (CAD) is often associated with delayed vascular healing, resulting from vascular inflammation and hypersensitivity to durable polymers and drugs. Therefore, DES design, materials, and coatings have been technologically revolutionized. Herein, we designed a novel abluminal groove-filled biodegradable polymer sirolimus-eluting stent (AGF-BP-SES), with a sirolimus content of only about one-third of traditional DES. The mechanical performances of AGF-BP-SES during compression and expansion were investigated. The pharmacokinetic (PK) profile of sirolimus was studied in the swine model. The in vivo efficacy of AGF-BP-SES was compared with that of Xience PRIME® stent. The results showed that AGF-BP-SES exhibited mechanical properties similar to traditional DES, including the rebound ratio of radial contraction/direction, rebound ratio of axial contraction/direction, and inhomogeneity of compression/expansion. Despite utilizing a reduced dose of sirolimus, AGF-BP-SES delivered sirolimus to the coronary artery in a controlled and efficient manner. The stent maintained a safe and effective local drug concentration without local or systemic risks. In the swine model, histopathological indicators predicted safety and biocompatibility of AGF-BP-SES. In conclusion, AGF-BP-SES maintained similar mechanical properties as other stents while reducing the drug-loading capacity, and showed a favorable safety and efficacy profile of the targeted DES.

Graphical Abstract

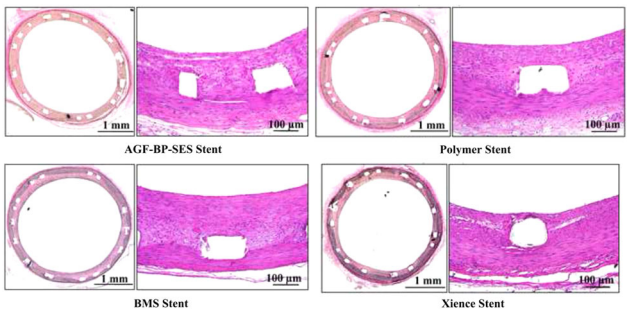

1 Introduction

Coronary artery disease (CAD), characterized by plaque build-up in the arteries, is the most common form of heart disease and the leading cause of death worldwide. Treatment options for CAD include bypass surgery and stent implantation, which utilizes small expandable mesh tubes to open the blocked arteries. Drug-eluting stents (DES) have shown excellent results in inhibiting neo-intimal hyperplasia compared with bare metal stents (BMS) in CAD patients [1]. However, late stent thrombosis (LST), defined as an

Electronic supplementary material The online version of this article (doi:10.1007/s10856-017-5864-0) contains supplementary material, which is available to authorized users.

✉ Chengli Song
csong@usst.edu.cn

✉ Ruiyan Zhang
rjzhangruiyan@aliyun.com

[1] Department of Cardiology, Rui Jin Hospital, School of Medicine, Shanghai Jiao Tong University, Shanghai 200025, China

[2] Shanghai Institute for Minimally Invasive Therapy, School of Medical Instrument and Food Engineering, Shanghai Science and Technology University, Shanghai 200093, China

acute thrombosis within a stent that has been in place for longer than 30 days, has emerged as a major cause of death and morbidity associated with DES [2, 3].

DES consists of three parts: a stent platform based on BMS; a spray-coated durable polymer; and an anti-proliferative drug. The polymer used in DES can hold and release the drug into the arterial wall by contact transfer [4]. However, both the durable polymer and drug can cause persistent inflammation of the vessel wall, thereby delaying endothelial healing and promoting LST [5]. Recent advances in DES technology aim to improve vascular healing, prevent restenosis, and reduce the risk of LST by developing bio-absorbable polymers and coating [6–9].

Herein, we designed a novel abluminal groove-filled biodegradable poly-lactic acid (PLA) polymer sirolimus-eluting stent (AGF-BP-SES). A formulation of sirolimus in a PLA polymer complex was poured into abluminal grooves in the outer surface of the cobalt-chromium alloy-based stent struts. The drug content is only about one-third of that in Cypher® (Johnson & Johnson, New Brunswick, NJ, USA). The biodegradable coating degraded over time, leaving a BMS. Our goal in this novel DES design was to reduce LST with preserved anti-restenosis activity. The aim of this study was to investigate the mechanical properties; examine the pharmacokinetic profile; and evaluate the safety and efficacy of this novel DES in a Chinese domestic swine coronary artery model.

2 Materials and Methods

2.1 Study device

The novel AGF-BP-SES consisted of three components: a cobalt-chromium L605 platform designed in S-type link (elastic modulus: 243 GPa, poisson ratio: 0.30) with total strut thickness of 86 μm; a biodegradable PLA polymer; and sirolimus, an anti-proliferative drug spayed into abluminal grooves. The unique abluminal grooves were scored at the outer surface of every "n" or "m" type support struts, with an average sirolimus dosage of 3 μg/mm stent lengths (Fig. 1). The parameters of the groove were finally set as length 510 μm, width 20 μm, depth 50 μm, based on previous studies.

2.2 Finite element (FE) analysis

Finite element analysis is used to address biomechanical problems, especially stress distribution [10, 11]. In the present study, the important mechanical properties of stents during compression and expansion were analyzed, including rebound ratio of radial contraction/direction, rebound ratio of axial contraction/direction, inhomogeneity of compression/expansion, and distribution of residual stress. Briefly, AGF-BP-SES and traditional stent with 3.03 mm in diameter and 18 mm in length were analyzed. Stent data were saved in Digital imaging and communication in medicine (Dicom), and entered into Solidworks 2012 (DS SolidWorks, Waltham, MA, USA). HyperMesh 10.1 (Altair Engineering, Troy, MI, USA) was used to mesh the models with a hexahedron mesh. The model was imported into the FE software (Abaqus 6.12, Simulia, Providence, RI, USA) for definition of the material properties.

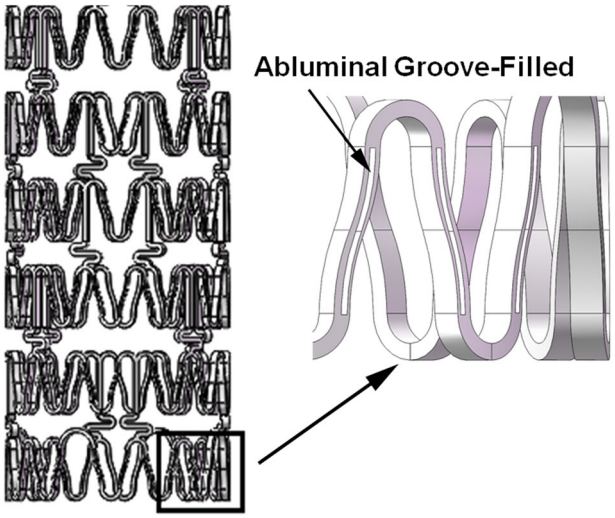

Fig. 1 Geometric model of AGF-BP-SES

Fatigue performance of stents was important for successful implantation of the coronary stent. Therefore, FE was used to analyze the fatigue strength of the stents by the Goodman curve.

2.3 In vivo pharmacokinetic study

Animal experiments were performed with the authorization of Animal Care and Use Committee of Shanghai Jiaotong University. Fifty-six Chinese domestic swine were randomly divided into two groups ($n = 28$ in each group). One group of animals were implanted with AGF-BP-SES (size: φ3.0 × 18 mm, labeled sirolimus content: 47 μg) and the other group with Cypher® (size: φ3.0 × 18 mm, labeled sirolimus content: 150 μg), all in left anterior descending artery. Three days before the procedure and throughout the follow-up period, all animals received oral administrations of 100 mg aspirin and 75 mg clopidogrel daily, which is the standard treatment administered to human patients with DES implantation. Animals were sacrificed after 1, 3, 7, 14, 30, 60, and 90 days of stent implantation, with $n = 4$ in each time point.

Whole blood and tissue samples were collected to determine the concentration of sirolimus. For coronary

artery samples collection, the stented coronary arterial segments were carefully dissected from the heart after removal from the thoracic cavity. The stented section plus 18 mm of adjacent proximal and distal non-stented tissue each were excised with micro-dissection scissors. The stents were carefully separated from the arterial tissue (luminal and abluminal) with blunt dissection. Samples were also taken from the left apical lung ($30 \times 10 \times 10$ mm), left lateral liver ($30 \times 10 \times 10$ mm), and left apical kidney ($20 \times 10 \times 10$ mm) to analyze the sirolimus concentration by tandem mass spectrometry analysis with AB Sciex API 4000 triple quadruple mass spectrometer (Foster City, CA, USA) equipped with a turbo ion spray source.

PK values were estimated using non-compartmental methods, including maximum observed blood concentration (C_{max}), time to Cmax (T_{max}), elimination half-life ($T_{1/2}$), apparent systemic clearance (CL/F), and area under the concentration-time curve (AUC).

2.4 In vivo safety and efficacy study

In experiment 1, Chinese domestic swine (weighing 55 to 90 kg) were randomly divided into AGF-BP-SES single stent (SS), Polymer SS, BMS SS, and Xience SS groups. They were followed for 3, 28, and 90 days. AGF-BP-SES SS group included swine with AGF-BP-SES, polymer SS included swine with AGF-BP-SES without drug eluting, and BMS SS group included swine with standard BMS. Xience SS referred to the Xience PRIME® DES (Abbott Vascular, Sana Clara, CA, USA). Animals were sedated and anesthetized with intravenous ketamine (20 mg/kg) and atropine (1 mg). Arterial access was achieved by a femoral artery cut-down, and nitroglycerin (100 μg) and heparin (100 IU/kg) were administered in the coronary vessels. Coronary angiography was performed using 6 F guiding catheters under digital subtraction angiography (INNOVA 2100, GE Healthcare, Little Chalfont, Buckinghamshire, United Kingdom). Stents were implanted in two major branches of the coronary artery: the left anterior descending and the right coronary artery. Three days before the procedure and throughout the follow-up period, all animals received oral administrations of 100 mg aspirin and 75 mg clopidogrel daily.

In experiment 2, Swine were randomly divided into AGF-BP-SES overlap (OL), Polymer OL, BMS OL, and Xience OL groups to study the overlap of stents on arterial healings. The swine were followed for 3, 28, or 90 days. The study protocol was as the same as in experiment 1. Arterial tissues with stent implants were harvested for histological and scanning electron microscopy (SEM).

2.5 Histological analysis

Hematoxylin and Eosin (H&E) was used to stain the stented arterial segments. The samples were dehydrated in ethanol and embedded in methylmethacrylate plastic. After polymerization, the stent section was cut on a rotary microtome (EXAKT, Norderstedt, Germany) into≈10 μm thickness and stained with H&E. An experienced pathologist, blinded to the groups, performed all histological analyses. Ordinal data were collected on each stent section, including lumen area, internal elastic membrane area, neointimal thickness, neointimal area, percent lumen stenosis, percent struts with fibrin, mean fibrin score, percent mal-apposition, percent endothelialization, injury score, and inflammation score. Neointimal thickness was measured as the distance from the inner surface of each stent strut to the luminal border. Percent-area stenosis was calculated as [1—(lumen area/internal elastic membrane area)] × 100. Vessel injury score was calculated according to the Schwartz method [12]. The inflammation score around the stent struts was measured as described previously [13].

2.6 SEM analysis

Though the Food and Drug Administration typically recommends 6-month data for preclinical stent data, 3-month follow-up is generally acceptable for initiating Investigational Device Exemption clinical trials if no adverse findings are noted at this time [14]. Thus, in the present study, stented vessels from each group obtained at 7, 28, and 90 days were examined en face by SEM for analysis of potential stent and late stent thrombosis incidence. Samples were fixed with 2.5% glutaraldehyde in 0.1 M sodium cacodylate buffer overnight and washed thrice with cacodylate buffer. Post-fixation was completed with 1% osmium tetroxide in 0.1 M cacodylate buffer, then serially dehydration with ethanol (30, 50, 70, 90, 95, and 100%), and critical point drying with CO_2. The samples were gold sputtered and visualized under SEM (Quanta 250, FEI, Hillsboro, OR, USA). Regions of interest were imaged at incremental magnifications.

2.7 Statistical analysis

Continuous variables were presented as mean ± standard deviation, and categorical variables were presented as counts and percentages. Paired comparisons were done using paired student's *t*-test. All statistical tests were two-tailed and a *p* value of less than 0.05 was considered statistically significant. WinNonlin software (version 6.2, PHARSIGHT Corporation, Mountain View, CA, USA) was used for the calculation of PK parameters. Statistical analyses were performed with SPSS 17.0 (IBM, Armonk, NY, USA).

3 Results

3.1 FE analysis results

At the same outer radius, AGF-BP-SES had mechanical performances similar to the control stent during compression and expansion. There were no significant differences in rebound ratio of radial contraction, rebound ratio of axial contraction, and inhomogeneity of compression between the two stents (Fig. S1). The rebound ratio of radial direction, rebound ratio of axial direction, and inhomogeneity of expansion did not differ in the two stents (Fig. S2). In contrast, AGF-BP-SES (Fig. S3A) had a larger low-stress area compared with the larger high-stress area in the control stent (Fig. S3B). Compared with the traditional DES, AGF-BP-SES maintained similar mechanical performance and reducing drug-loading capacity, suggesting its potential clinical applicability in cardiovascular stenosis diseases.

For fatigue analysis, the high-stress area is always located in the arc sections during the deformation process. Our results showed that as all the feature points of the two stents were located under the fatigue limit line, which indicated that stent crash was not possible after implantation (AGF-BP-SES in Fig. S4A and control stent in Fig. S4B). Moreover, there was a negative correlation between the safety factor and stent length, width, and thickness of AGF-BP-SES (Fig. S4C–E).

3.2 Pharmacokinetic application

The PK parameters 72 h after the implantation of AGF-BP-SES or Cypher® stents in swine blood are summarized in Table 1. The concentration profile is shown in Fig. 2a. These data indicated that systemic exposure to the drug in terms of AUC was lower with AGF-BP-SES compared with the Cypher® stent. There was no significant difference in terms of T_{max} and $T_{1/2}$ between the two groups. For the apparent total systemic clearance (CL/F), sirolimus was eliminated faster in the AGF-BP-SES group than the Cypher® stent group.

Drug concentration was measured in the arteries, myocardium, kidney, lung, and liver. The peak sirolimus concentration after AGF-BP-SES implantation occurred at Day 1 with a mean of 3555 ± 1225 ng/g and decreased to 1713 ± 493 ng/g by Day 90. After Cypher® stent implantation, sirolimus levels were maintained from 6896 ± 3412 to 328 ± 335 ng/g from Day 1 to Day 90. The drug concentration in AGF-BP-SES group decreased slowly during 30 days post implantation and achieved similar concentration to that in Cypher® group on Day 30 (Fig. 2b). From Day 30 to Day 90, the concentrations of sirolimus in AGF-BP-SES group remained constant, which indicated that the drug reached equilibrium. Peak levels of sirolimus in the proximal and distal non-stented segments were less than 5% of that in the stented segments. As expected, sirolimus levels in distal vessel segments were greater than in the proximal segments. Sirolimus level in the myocardium subjacent to the stented artery in the AGF-BP-SES group was 76.3 ± 44.2 ng/g on Day 1 and decreased to 0.64 ± 0.32 ng/g after 90 days, compared with 360 ± 264 ng/g (Day 1) and 0.51 ± 0.20 ng/g (Day 90) in the Cypher® group. Similarly, sirolimus levels in the distal myocardium were higher than those in the proximal segments. The drug levels in the liver, lung, and kidney were measurable up to 14–28 days after stent implantation, with peak levels between 0.25 and 1.85 ng/g in AGF-BP-SES group and 0.23 to 12.0 ng/g in Cypher® group (Fig. 2c).

Table 1 Calculated pharmacokinetic parameters of stented swine (blood) ($T = 72$ h)

PK parameter	AGF-BP-SES (Dosage: 94 μg, $n = 4$)	Cypher (Dosage: 300 μg, $n = 4$)
T_{max} (h)	2.25 ± 0.29	2.00 ± 0.50
C_{max} (pg/mL)	786 ± 246	2496 ± 441
$AUC_{0\text{-}t}$ (pg•h/mL)	14630 ± 4628	63873 ± 8425
$AUC_{0\text{-}\infty}$ (pg•h/mL)	22640 ± 8704	107120 ± 7557
$T_{1/2}$ (h)	50.4 ± 11.2	55.5 ± 8.42
CL/F (mL/h)	6913 ± 2066	4757 ± 673

The PK parameters are provided in Table 2. The parameters showed that the AUC of arterial tissue with stent was 192,048 ng•day/g in AGF-BP-SES group and 185,368 ng•day/g in Cypher® group. However, the AUC in other tissues was far lower (1/2–1/5) than in the Cypher® group. The lower concentration of the drug in peripheral tissues suggested that AGF-BP-SES had a similar mechanism of action but reduced side effects.

Lung toxicity is a serious complication associated with sirolimus [15, 16]. However, sirolimus was detected at very low levels in the lungs in this study (the C_{max} is about 2.00 ng/g; 0.20 ng/g at 30 days).

After AGF-BP-SES implantation, the mean percentage of cumulatively released sirolimus was 21% in 24 h, 59% at 7 days, 72 at 28 days, 85 at 60 days, and 90% at 90 days. These values were statistically similar to those released in the Cypher® group: 9, 27, 46, 61, 78, 88, and 95% in the, respectively (Fig. 2d).

3.3 Histomorphometry and histology

The in vivo safety and efficacy of the AGF-BP-SES was evaluated by the histological analysis of stented arteries with or without overlap in swine. The results are summarized in Tables 3 and 4.

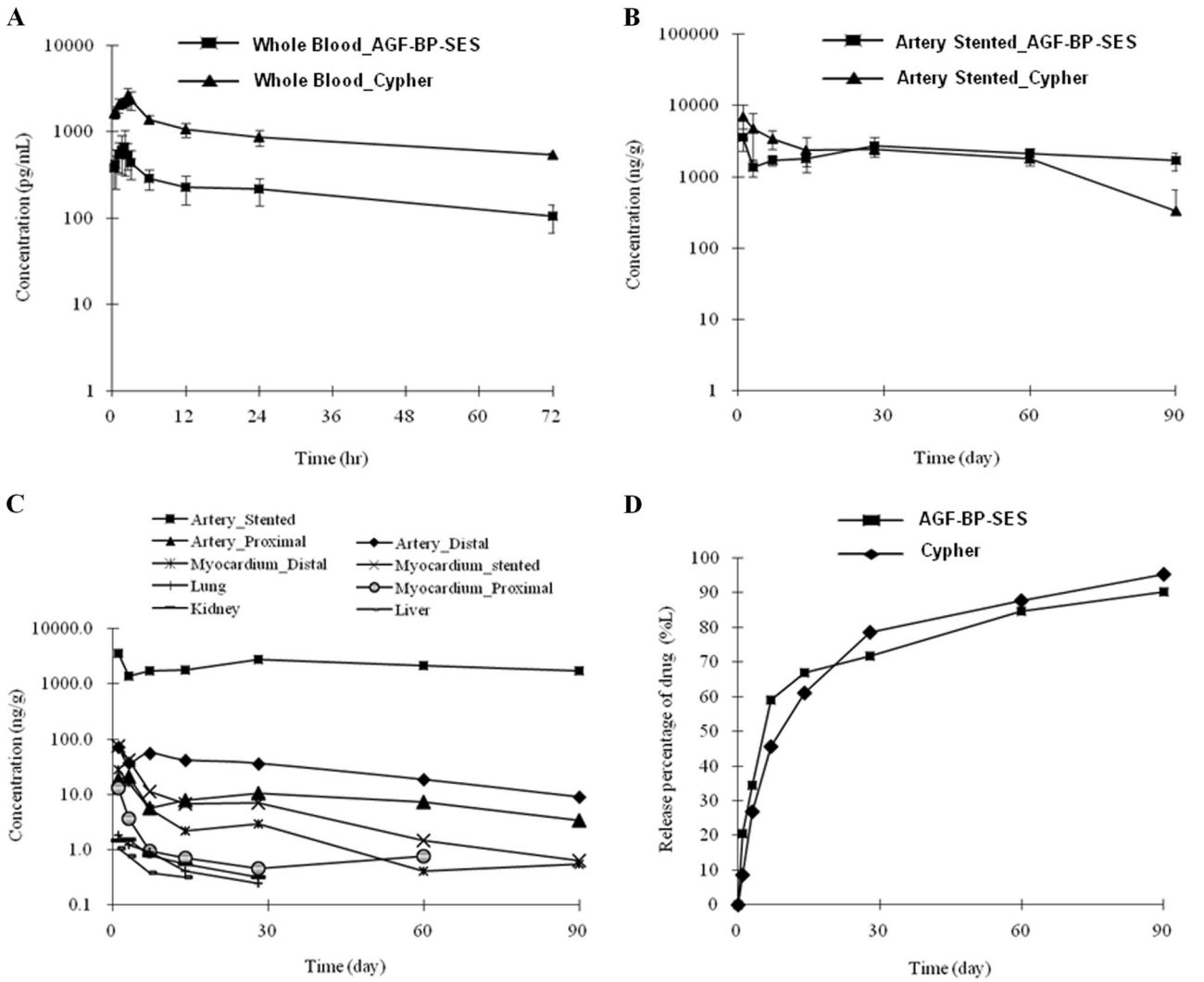

Fig. 2 Mean sirolimus whole blood concentration-time profiles in swine after implanting AGF-BP-SES or Cypher® **a**. Mean sirolimus stented artery concentration-time profiles in swine after implanting AGF-BP-SES or Cypher® **b**. Mean sirolimus tissues concentration-time profiles in swine after implanting AGF-BP-SES **c**. In vitro release profile of sirolimus from AGF-BP-SES and Cypher® stent **d**. Data points presented as mean ± SD

All 25 animals survived the 3-day study duration. Histologically, malapposition was not observed in any section. Analysis of morphometric data showed similar vessel area (EEL, IEL, lumen) in both single and overlapping stents from all groups. Neointimal/thrombus areas and stenosis percentage in single stents were lowest with Xience SS and highest with BMS SS (Table 3). In overlapping stents, the stenosis percentage was lowest with Xience OL (Table 4). The majority of struts in all groups were surrounded by significant fibrin deposition, which, at this early duration, was characterized as thrombus burden with frequent intermixed platelets and red blood cells, and an incomplete endothelial layer. Generally, mean fibrin scores were similar between groups (single and overlapping). Percentage of total struts with surrounding fibrin was highest with BMS SS and lowest with Xience SS. In overlapping groups, both AGF-BP-SES OL and BMS OL showed a significantly greater percentage of struts with fibrin than with Xience OL. Inflammation was generally mild for all stent groups, with the least inflammation seen with Xience (single and overlapping) and most with BMS (single and overlapping). Mean injury scores were minimal and statistically comparable among all overlapping groups. In SS, however, AGF-BP-SES, Polymer SS, and Xience SS showed significantly reduced injury than BMS SS. In all groups, endothelialization of luminal surfaces by light microscopy was incomplete with frequent adherent luminal inflammatory cells and platelets. In SS groups endothelialization was similar, with Polymer SS showing slightly greater endothelialization than others. In overlapping stents, however, BMS OL showed significantly greater endothelialization than other groups (Fig. 3).

Table 2 Calculated pharmacokinetic parameters of stented swine in different tissues ($T = 90$ day)

Tissue	PK parameter	AGF-BP-SES ($n = 4$)	Cypher ($n = 4$)
Blood	T_{max} (Day)	1	1
	C_{max} (pg/mL)	113	733
	$AUC_{0\text{-}t}$ (pg•day/mL)	615	6776
Artery (stent)	T_{max} (Day)	1	1
	C_{max} (ng/g)	3555	6896
	$AUC_{0\text{-}t}$ (ng•day/g)	192048	185369
Artery (proximal)	T_{max} (Day)	3	1
	C_{max} (ng/g)	21	99
	$AUC_{0\text{-}t}$ (ng•day/g)	732	875
Artery (distal)	T_{max} (Day)	1	1
	C_{max} (ng/g)	72.6	255
	$AUC_{0\text{-}t}$ (ng•day/g)	2540	5768
Myocardium (stent)	T_{max} (Day)	1	1
	C_{max} (ng/g)	76.3	360
	$AUC_{0\text{-}t}$ (ng•day/g)	594	1817
Myocardium (proximal)	T_{max} (Day)	1	3
	C_{max} (ng/g)	13.0	17.8
	$AUC_{0\text{-}t}$ (ng•day/g)	97.7	170
Myocardium (distal)	T_{max} (Day)	1	1
	C_{max} (ng/g)	28.2	186
	$AUC_{0\text{-}t}$ (ng•day/g)	234	1088
Kidney	T_{max} (Day)	3	1
	C_{max} (ng/g)	1.51	12.0
	$AUC_{0\text{-}t}$ (ng•day/g)	19.2	106
Liver	T_{max} (Day)	1	1
	C_{max} (ng/g)	1.06	6.13
	$AUC_{0\text{-}t}$ (ng•day/g)	7.16	62.5
Lung	T_{max} (Day)	1	1
	C_{max} (ng/g)	1.85	8.72
	$AUC_{0\text{-}t}$ (ng•day/g)	17.5	77.3

All 41 animals survived to the 28-day study time-point. Histologically, all devices showed good apposition to the vessel wall with uniform expansion. Analysis of morphometric data showed similar EEL and IEL areas in both single and overlapping stents from all groups. Lumen areas in overlapping stents, however, were smallest with Polymer OL and largest with Xience OL. Neointimal areas and stenosis percentage were statistically similar in single stents, but were lowest in AGF-BP-SES OL in overlapping stents. Fibrin deposition was moderate and surrounded the majority of struts in both single and overlapping AGF-BP-SES groups. Both Polymer and BMS groups (single and overlapping) had significantly less fibrin than AGF-BP-SES. Mean injury scores are minimal and statistically comparable among all groups (single and overlapping). Endothelialization of luminal surfaces by light microscopy was near complete in all groups with occasional adherent luminal inflammatory cells (Fig. 4).

Forty-one of the 43 animals survived the 90-day study duration. There were two early deaths: one on the day of implantation and the other euthanized during implantation due to ventricular fibrillation. Histologically, all devices showed good apposition to the vessel wall with uniform expansion. Malapposition was not seen in any section. Analysis of morphometric data showed significantly greater EEL areas in BMS SS compared with AGF-BP-SES SS. All other morphometric measurements (including IEL, lumen, and medial area) were similar in both single and overlapping stents from all groups. Neointimal areas and stenosis percentage were statistically similar between groups in single and overlapping stents. Fibrin deposition was mild and frequently seen surrounding struts in single and overlapping groups. Mean injury scores were minimal and statistically comparable among all groups (single and overlapping). Endothelialization of luminal surfaces by light microscopy was near complete in all groups with occasional adherent luminal inflammatory cells (Fig. 5).

3.4 SEM analysis

SEM analysis showed good expansion of all stents at 3, 28, and 90 days. The majority of stent surfaces showed incomplete coverage by endothelium at day 3, but near complete coverage at days 28 and 90. All stent groups showed regions of fibrin/platelet thrombi on strut surfaces with frequent inflammatory cells. None of the groups showed obstructive luminal thrombi. Similar coverage was seen between all groups. Representative images of AGF-BP-SES and Xience Prime are shown in Fig. 6.

4 Discussion

The deformation process of balloon-expansible coronary stents occurs in three stages: compression towards the balloon when the stents are assembling; expansion under the force exerted by the balloon; and periodic compression of the vascular wall after the balloon was removed. In this study, we designed a novel abluminal groove-filled biodegradable PLA polymer sirolimus-eluting stent (AGF-BP-SES), which

Table 3 Morphometric comparison of cross-sectional vessel areas and neointimal thickness

Implant group	AGF-BP-SES SS	Polymer SS	BMS SS	Xience SS
Day 3	$n = 6$	$n = 6$	$n = 6$	$n = 6$
Injury score	0.016 ± 0.039^{a}	0.00 ± 0.00^{a}	0.087 ± 0.074	0.009 ± 0.021^{a}
Inflammation score	0.67 ± 0.42^{a}	1.00 ± 0.60	1.39 ± 0.53	0.44 ± 0.34^{a}
Struts with fibrin (%)	74.61 ± 15.15	64.44 ± 15.88	92.82 ± 6.77	47.81 ± 29.78^{a}
Mean fibrin score	1.33 ± 0.42	1.33 ± 0.37	1.89 ± 0.27	1.33 ± 0.79
Malapposition (%)	0.00 ± 0.00	0.00 ± 0.00	0.00 ± 0.00	0.00 ± 0.00
EEL area (mm^2)	9.33 ± 1.96	9.15 ± 1.68	8.99 ± 2.49	9.31 ± 1.28
IEL area (mm^2)	8.58 ± 1.82	8.45 ± 1.56	8.20 ± 2.31	8.20 ± 1.13
Lumen area (mm^2)	8.14 ± 1.78	7.96 ± 1.49	7.58 ± 2.31	8.19 ± 1.03
Medial area (mm^2)	0.75 ± 0.16	0.70 ± 0.12	0.78 ± 0.20	0.81 ± 0.18
N/T area (mm^2)	0.47 ± 0.10	0.48 ± 0.15	0.62 ± 0.13	0.31 ± 0.20
N/T thickness (mm)	0.012 ± 0.006^{a}	0.015 ± 0.011	0.023 ± 0.014	0.008 ± 0.010^{a}
Stenosis (%)	5.22 ± 1.28^{a}	5.69 ± 1.47	8.03 ± 2.91	3.53 ± 2.10^{a}
Endothelialization	25.56 ± 12.72	36.67 ± 10.27^{a}	29.44 ± 8.80	21.94 ± 14.47
Day 28	$n = 10$	$n = 10$	$n = 10$	$n = 10$
Injury score	0.096 ± 0.150	0.069 ± 0.090	0.120 ± 0.160	0.230 ± 0.370
Inflammation score	0.00 ± 0.00	0.13 ± 0.32	0.07 ± 0.14	0.10 ± 0.22
Struts with fibrin (%)	90.23 ± 9.84	64.58 ± 22.84	38.96 ± 19.65	92.93 ± 5.71
Mean fibrin score	1.60 ± 0.34^{a}	1.03 ± 0.40	0.73 ± 0.44	1.70 ± 0.51^{a}
Malapposition (%)	0.26 ± 0.81	0.00 ± 0.00	0.00 ± 0.00	1.84 ± 3.85
EEL area (mm^2)	8.74 ± 1.97	9.74 ± 1.54	8.68 ± 1.68	9.10 ± 0.86
IEL area (mm^2)	7.52 ± 1.73	8.39 ± 1.37	7.54 ± 1.53	7.84 ± 0.87
Lumen area (mm^2)	6.29 ± 1.57	6.76 ± 1.43	5.95 ± 1.56	6.34 ± 0.82
Medial area (mm^2)	1.22 ± 0.36	1.35 ± 0.25	1.14 ± 0.22	1.26 ± 0.25
N/T area (mm^2)	1.23 ± 0.43	1.63 ± 0.47	1.59 ± 0.28	1.50 ± 0.56
N/T thickness (mm)	0.080 ± 0.039	0.120 ± 0.064	0.130 ± 0.050	0.110 ± 0.062
Stenosis (%)	16.50 ± 4.62	19.80 ± 6.38	21.86 ± 6.21	18.99 ± 6.26
Endothelialization	98.40 ± 1.27	99.33 ± 0.42	98.67 ± 1.34	97.57 ± 2.86
Day 90	$n = 10$	$n = 10$	$n = 10$	$n = 10$
Injury score	0.270 ± 0.360	0.079 ± 0.120	0.130 ± 0.130	0.300 ± 0.380
Inflammation score	0.430 ± 0.890	0.033 ± 0.110	0.170 ± 0.360	0.630 ± 1.250
Struts with fibrin (%)	45.02 ± 17.76	5.64 ± 7.38	0.72 ± 1.66	46.04 ± 27.28
Mean fibrin score	0.70 ± 0.29	0.033 ± 0.11	0.00 ± 0.00	0.83 ± 0.63
Malapposition (%)	0.00 ± 0.00	0.00 ± 0.00	0.00 ± 0.00	0.00 ± 0.00
EEL area (mm^2)	7.89 ± 1.42^{a}	8.70 ± 0.79	9.27 ± 0.82	8.12 ± 1.17
IEL area (mm^2)	6.81 ± 1.29	7.29 ± 0.58	7.91 ± 0.93	6.97 ± 0.96
Lumen area (mm^2)	5.26 ± 1.43	5.89 ± 0.66	6.30 ± 1.07	5.39 ± 0.83
Medial area (mm^2)	1.07 ± 0.19	1.41 ± 0.37	1.36 ± 0.33	1.15 ± 0.25
N/T area (mm^2)	1.55 ± 0.48	1.40 ± 0.23	1.61 ± 0.42	1.59 ± 0.61
N/T thickness (mm)	0.120 ± 0.062	0.092 ± 0.025	0.120 ± 0.059	0.130 ± 0.068
Stenosis (%)	23.72 ± 8.21	19.34 ± 3.72	20.68 ± 5.95	22.51 ± 7.23
Endothelialization	99.67 ± 0.24	99.89 ± 0.24	100.0 ± 0.00	99.67 ± 0.57

Analysis includes mean of all sections (proximal, mid, and distal stented sections)

N/T neointimal/thrombus

[a] $P < 0.05$ vs. BMS SS

Table 4 Morphometric comparison of cross-sectional vessel areas and neointimal thickness

Implant group	AGF-BP-SES OL	Polymer OL	BMS OL	Xience OL
Day 3	$n = 6$	/	$n = 6$	$n = 6$
Injury score	0.072 ± 0.083	/	0.032 ± 0.033	0.130 ± 0.160
Inflammation score	0.83 ± 0.34[a]	/	1.32 ± 0.28	0.79 ± 0.19[a]
Struts with fibrin (%)	91.33 ± 9.45	/	91.08 ± 10.43	71.60 ± 10.87[a]
Mean fibrin score	2.13 ± 0.54	/	1.99 ± 0.29	1.75 ± 0.47
Malapposition (%)	0.00 ± 0.00	/	0.00 ± 0.00	0.00 ± 0.00
EEL area (mm^2)	8.65 ± 2.05	/	7.96 ± 1.63	9.50 ± 1.07
IEL area (mm^2)	7.83 ± 1.80	/	7.20 ± 1.54	8.76 ± 0.95
Lumen area (mm^2)	7.22 ± 1.70	/	6.59 ± 1.53	8.26 ± 0.95
Medial area (mm^2)	0.82 ± 0.25	/	0.76 ± 0.13	0.75 ± 0.16
N/T area (mm^2)	0.62 ± 0.19	/	0.60 ± 0.04	0.49 ± 0.11
N/T thickness (mm)	0.012 ± 0.004	/	0.015 ± 0.003	0.014 ± 0.007
Stenosis (%)	7.96 ± 2.21	/	8.64 ± 1.69	5.63 ± 1.31[a]
Endothelialization	16.04 ± 8.19[a]	/	44.68 ± 21.87	13.54 ± 6.44[a]
Day 28	$n = 10$	$n = 10$	$n = 10$	$n = 10$
Injury score	0.075 ± 0.080	0.140 ± 0.190	0.065 ± 0.100	0.140 ± 0.130
Inflammation score	0.050 ± 0.110	0.068 ± 0.230	0.230 ± 0.340	0.083 ± 0.140
Struts with fibrin (%)	85.27 ± 14.87	55.03 ± 20.12	34.39 ± 16.43	89.27 ± 11.48
Mean fibrin score	1.60 ± 0.36[a]	1.02 ± 0.21	0.68 ± 0.40	1.58 ± 0.41[a]
Malapposition (%)	0.00 ± 0.00	0.00 ± 0.00	0.00 ± 0.00	0.38 ± 1.22
EEL area (mm^2)	8.45 ± 1.61	8.35 ± 1.16	8.71 ± 1.15	9.31 ± 1.28
IEL area (mm^2)	7.34 ± 1.44	7.22 ± 1.04	7.56 ± 1.01	8.03 ± 1.12
Lumen area (mm^2)	5.84 ± 1.14	4.98 ± 1.01[a]	5.40 ± 0.82	6.32 ± 1.19[a]
Medial area (mm^2)	1.11 ± 0.20	1.13 ± 0.19	1.15 ± 0.18	1.27 ± 0.22
N/T area (mm^2)	1.50 ± 0.38[a]	2.24 ± 0.62	2.16 ± 0.57	1.71 ± 0.46
N/T thickness (mm)	0.070 ± 0.024[a]	0.170 ± 0.086	0.140 ± 0.056	0.110 ± 0.047[a]
Stenosis (%)	20.47 ± 2.85[a]	30.97 ± 8.09	28.51 ± 5.65	21.45 ± 5.94[a]
Endothelialization	96.10 ± 3.95	99.20 ± 0.89	99.39 ± 0.47	98.53 ± 1.04
Day 90	$n = 10$	$n = 10$	$n = 10$	$n = 9$
Injury score	0.0 ± 0.080	0.120 ± 0.170	0.110 ± 0.120	0.340 ± 0.440
Inflammation score	0.050 ± 0.110	0.430 ± 0.860	0.050 ± 0.160	0.690 ± 1.130
Struts with fibrin (%)	38.70 ± 15.56	8.31 ± 4.75	3.56 ± 3.23	40.45 ± 30.85
Mean fibrin score	0.63 ± 0.24	0.16 ± 0.14	0.05 ± 0.11	0.68 ± 0.44
Malapposition (%)	0.00 ± 0.00	0.75 ± 2.37	0.00 ± 0.00	0.00 ± 0.00
EEL area (mm^2)	8.40 ± 1.31	8.95 ± 1.45	8.85 ± 1.27	8.28 ± 0.73
IEL area (mm^2)	7.12 ± 1.06	7.56 ± 1.22	7.55 ± 1.17	7.08 ± 0.75
Lumen area (mm^2)	5.13 ± 0.92	5.37 ± 0.98	5.55 ± 0.82	5.12 ± 0.76
Medial area (mm^2)	1.28 ± 0.37	1.39 ± 0.37	1.30 ± 0.31	1.20 ± 0.19
N/T area (mm^2)	2.00 ± 0.42	2.19 ± 0.66	2.00 ± 0.78	1.96 ± 0.35
N/T thickness (mm)	0.130 ± 0.055	0.160 ± 0.074	0.120 ± 0.084	0.140 ± 0.045
Stenosis (%)	28.11 ± 4.78	28.67 ± 6.99	26.05 ± 6.65	27.63 ± 5.14
Endothelialization	99.92 ± 0.13	99.86 ± 0.25	99.75 ± 0.56	99.38 ± 0.71

Analysis includes mean of all sections (proximal, mid1, mid2, and distal stented sections)

N/T neointimal/thrombus

[a] $P < 0.05$ vs. BMS OL

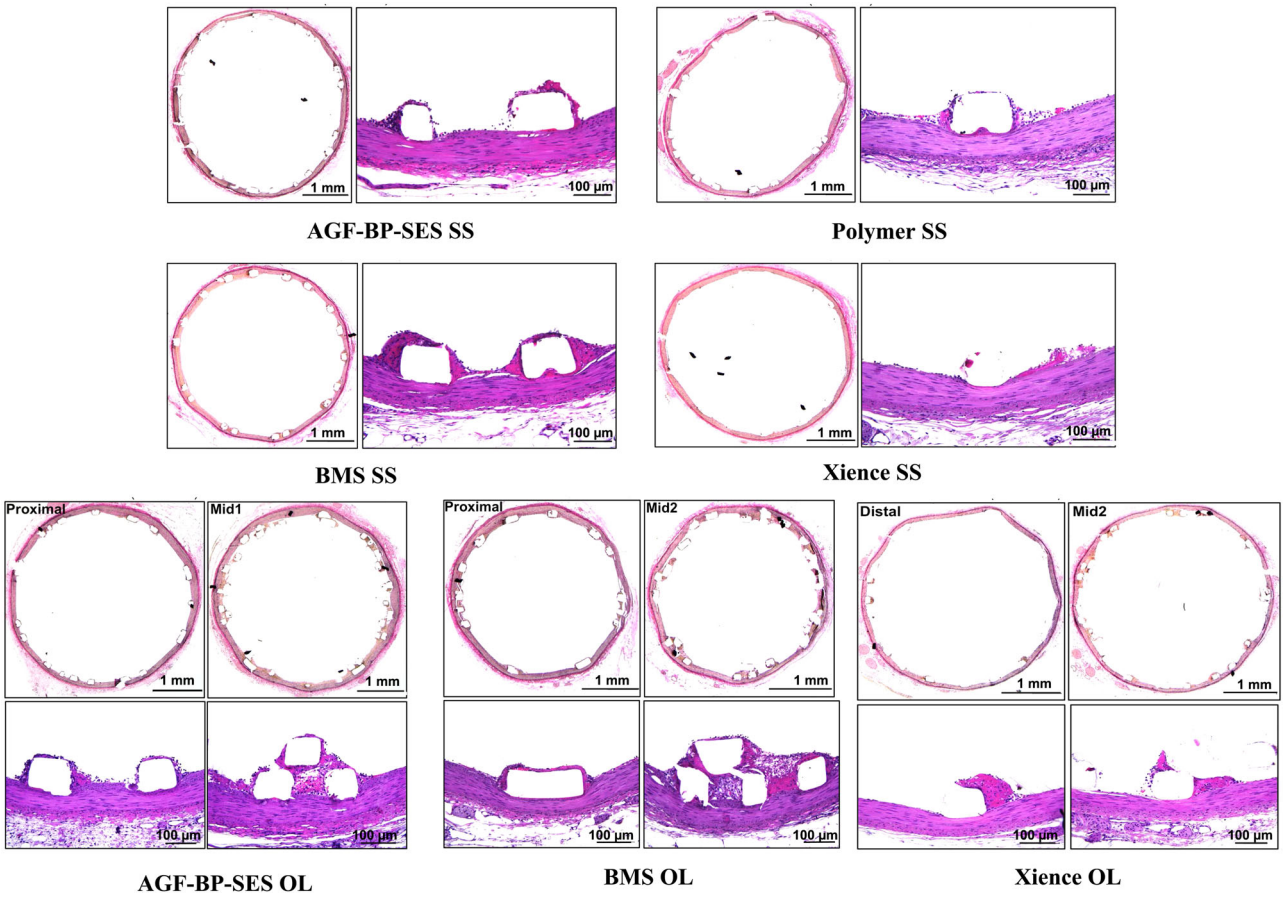

Fig. 3 Representative histological images at low- (×100) and high-magnification (×200) of different stents implanted into arteries at 3 days. There is moderate, localized aggregation of inflammatory cells adjacent to the lumen surface of the strut in all groups

was shown to have similar mechanical performance, including compression and expansion, compared with traditional DES.

In the in vivo preclinical PK study, sirolimus concentration at the stented coronary artery segment was much higher than that at the myocardium. The drug concentration in whole blood, liver, kidney, and lung was lower than in the myocardium, indicating that sirolimus from AGF-BP-SES was delivered to the stented coronary artery segment. The drug elimination rates in AGF-BP-SES group were shorter than the Cypher® group. These data support the systemic safety of AGF-BP-SES. The average drug concentration at the stented coronary artery segment was within the known therapeutic drug concentration range, and the peak drug concentration was much lower than the maximum acceptable drug concentration. Therefore, local tolerance and safety of AGF-BP-SES was evident. Local drug concentrations with AGF-BP-SES over time were evenly distributed within the therapeutic drug concentration range. During rapid proliferation phase of smooth muscle cells (SMCs), AGF-BP-SES delivers a drug amount to the stented coronary artery wall similar to that delivered by Cypher®. Consequently, the efficacy of AGF-BP-SES was clear.

DES significantly reduces restenosis and the need for repeat target lesion revascularization (TLR) [17]. Unfortunately, DES-based therapies contribute to the higher incidence of LST because of delayed healing and/or incomplete RE compared with BMS [18, 19]. In fact, recent studies suggest that the best predictor of LST is the ratio of uncovered/total stent struts [20]. A severe localized hypersensitivity reaction to polymer carriers can produce chronic inflammation and delay endothelialization, a major risk factor for LST [21–23]. Biodegradable polymers appear to be safer than non-biodegradable polymers because inflammation subsides with the degradation of the polymer [24]. A new generation biodegradable polymer DES that dissolves 6–9 months after implantation reduces the risk of late and very late stent thrombosis [7, 25, 26]. Lupi A et al. found that in comparison with biodegradable polymer DES, non-biodegradable polymer DES showed lower LLL and LST, but did not reduce mortality or TLR [27]. DES combines a PLA-based scaffold with an anti-proliferative drug, and appears to be feasible and effective in animal and human

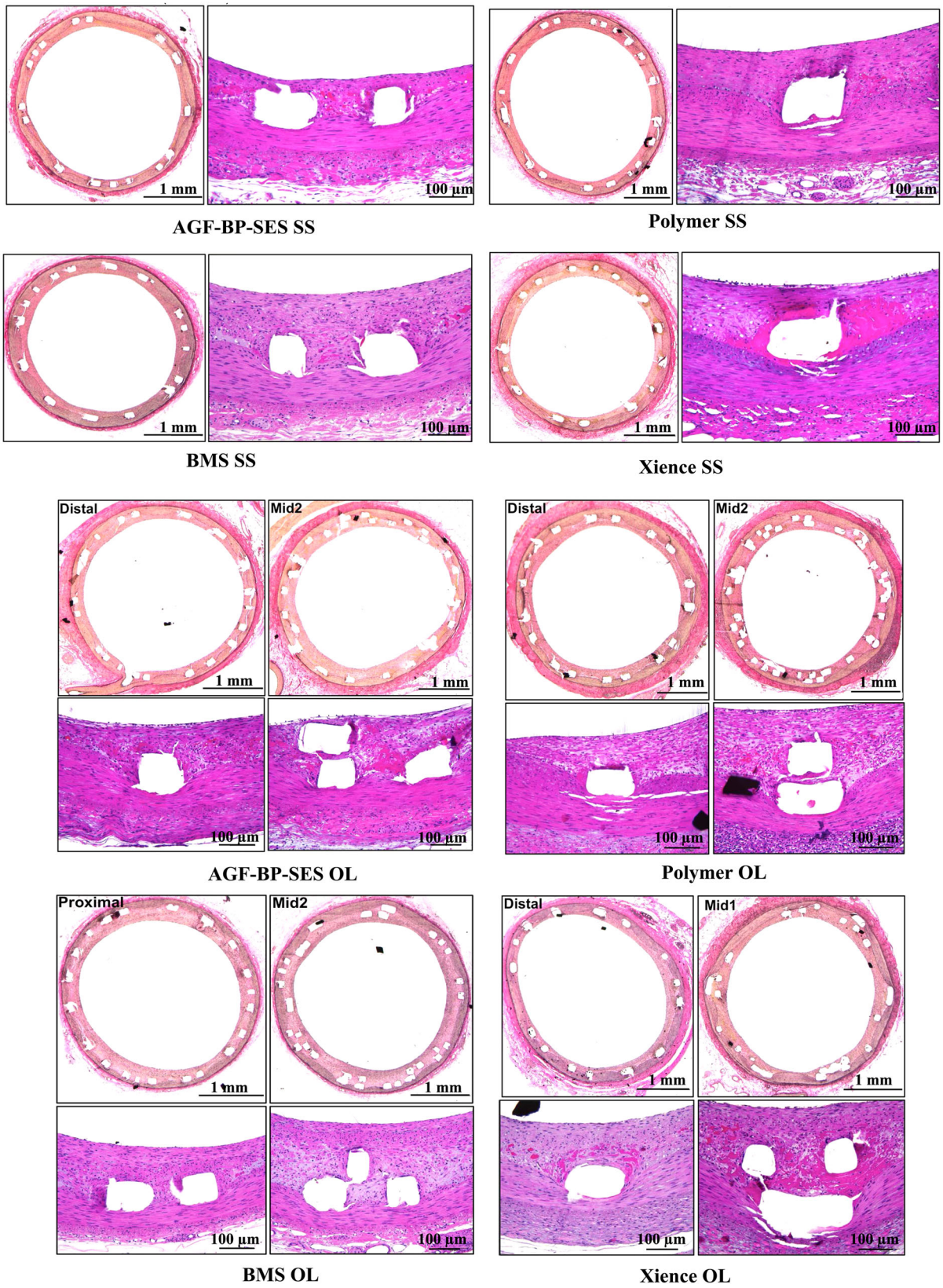

Fig. 4 Representative histological images at low- (×100) and high-magnification (×200) of different stents implanted into arteries at 28 days. Inflammatory scores were similar among the AGF-BP-SS, BMS, Polymer, and Xience groups. All stent groups exhibited normal neointima formation over the struts, including normal amount of smooth muscle cells with no histiocytes or lymphocytes

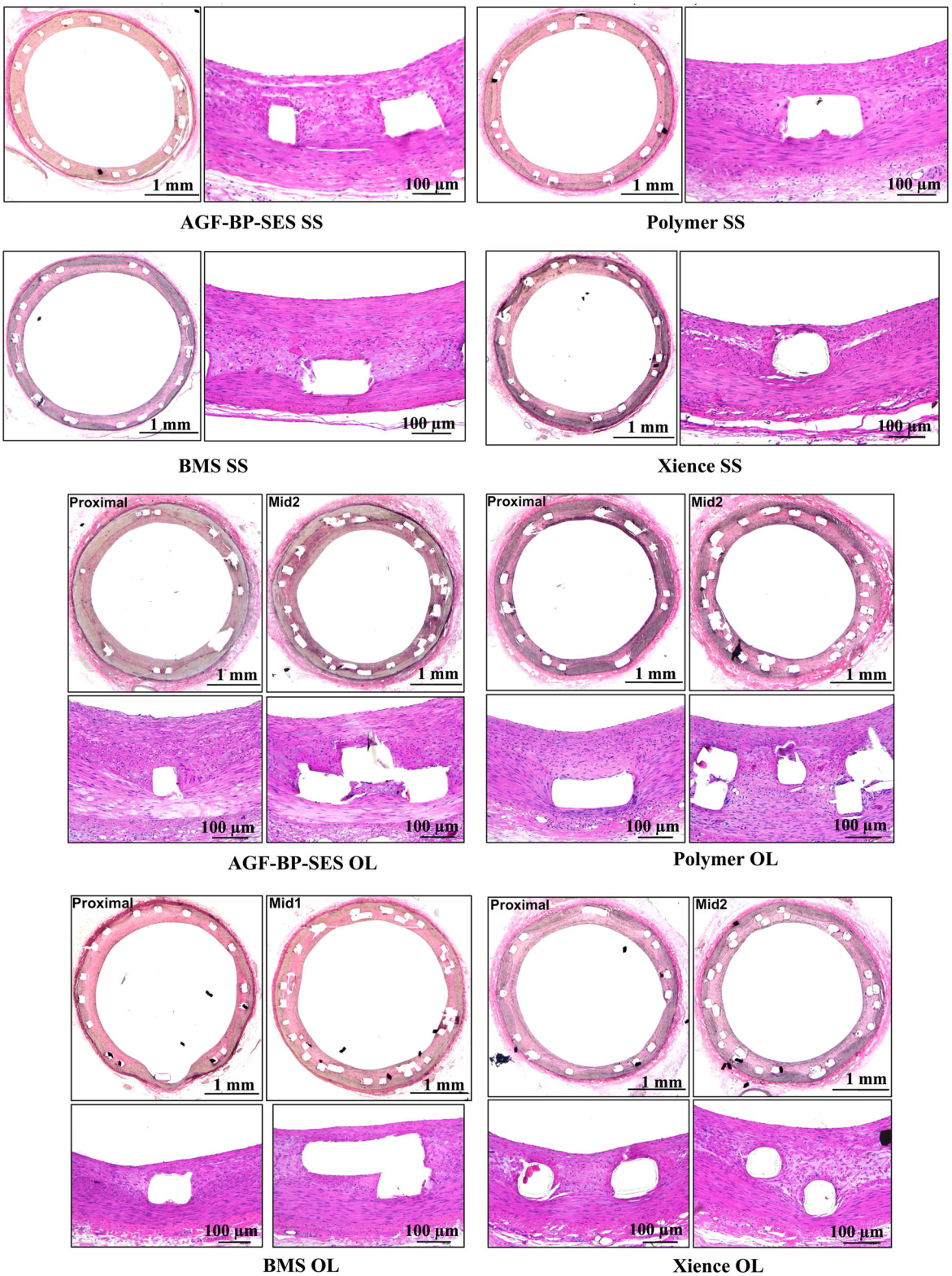

Fig. 5 Representative histological images at low- (×100) and high-magnification (×200) of different stents implanted into arteries at 90 days

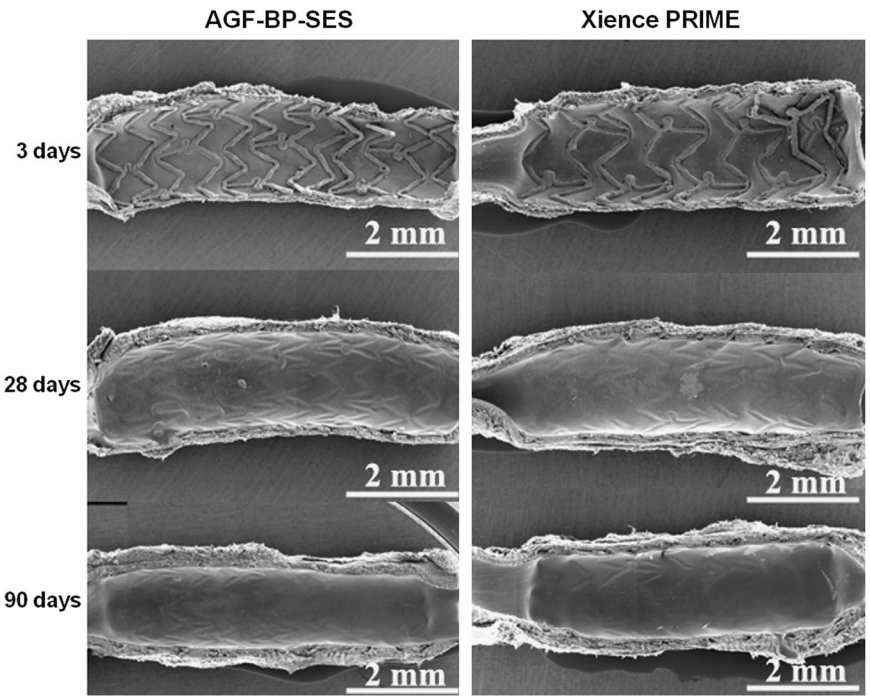

Fig. 6 Representative SEM Images of AGF-BP-SS vs. Xience PRIME in the swine coronary artery at different time-points. Endothelialization of luminal surfaces is incomplete with frequent adherent luminal inflammatory cells and platelets in both groups at day 3. However, endothelialization is near complete in both groups at day 28 and day 90

studies [28–30]. In the present study, we evaluated AGF-BP-SES with PLA polymer coating and compared it with standard DES and BMS at 3, 28, and 90 days after implantation. We showed that AGF-BP-SES successfully delivered the drug and demonstrated similar ability to inhibit long-term neointimal hyperplasia. Furthermore, AGF-BP-SES showed reduced inflammation within the vessel wall and better ability to preserve RE, thus had the potential to prevent LST.

Drug concentrations on the polymer of DES are also considered a risk factor for LST due to delay in endothelium healing [10]. Therefore, DES with abluminal coating has been developed [31, 32]. To minimize drug concentrations in the vessel, sirolimus and PLA polymer matrix are applied to the abluminal surface with a groove facing the vessel wall. This unique design reduces the drug concentration by targeting the vessel wall and minimizes long-term inflammation, decreases the stent thrombosis rate, yet maintains the anti-restenotic effect. The average sirolimus dosage of AGF-BP-SES was 3 μg/mm stent length, which was approximately one-third of standard stents. AGF-BP-SES inhibited long-term neointimal hyperplasia in animals similar to DES but was more efficacious in reducing inflammation, indicating that AGF-BP-SES had better ability to prevent LST.

In conclusion, we designed a novel targeted DES, AGF-BP-SES, which delivered sirolimus to the coronary artery segment in a controlled and efficient manner. There was a low risk of local and systemic risks as demonstrated in the animal studies.

Acknowledgements This work was supported by the Science and Technology Commission of Shanghai Municipality (grant 12441903200).

Compliance with ethical standards

Conflict of interest The authors declare that they have no competing interest.

References

1. Morice MC, Serruys PW, Sousa JE, Fajadet J, Ban Hayashi E, Perin M, Colombo A, Schuler G, Barragan P, Guagliumi G, Molnar F, Falotico R. A randomized comparison of a sirolimus-eluting stent with a standard stent for coronary revascularization. N Engl J Med. 2002;346:1773–80.
2. Ong AT, Hoye A, Aoki J, van Mieghem CA, Rodriguez Granillo GA, Sonnenschein K, Regar E, McFadden EP, Sianos G, van der Giessen WJ, de Jaegere PP, de Feyter P, van Domburg RT, Serruys PW. Thirty-day incidence and six-month clinical outcome of thrombotic stent occlusion after bare-metal, sirolimus, or paclitaxel stent implantation. J Am Coll Cardiol. 2005;45:947–53.
3. Zimarino M, Renda G, Maddestra N, De Caterina R. Late coronary thrombosis after drug-eluting stent: stent vs patient-driven prescription of aspirin-clopidogrel combination. Thromb Haemost. 2004;92:668–9.
4. Fattori R, Piva T. Drug-eluting stents in vascular intervention. Lancet. 2003;361:247–9.
5. Ong AT, McFadden EP, Regar E, de Jaegere PP, van Domburg RT, Serruys PW. Late angiographic stent thrombosis (LAST) events with drug-eluting stents. J Am Coll Cardiol. 2005;45:2088–92.
6. Stefanini GG, Kalesan B, Serruys PW, Heg D, Buszman P, Linke A, Ischinger T, Klauss V, Eberli F, Wijns W, Morice MC, Di Mario C, Corti R, Antoni D, Sohn HY, Eerdmans P, van Es GA, Meier B, Windecker S, Juni P. Long-term clinical outcomes of

biodegradable polymer biolimus-eluting stents versus durable polymer sirolimus-eluting stents in patients with coronary artery disease (LEADERS): 4 year follow-up of a randomised non-inferiority trial. Lancet. 2011;378:1940–8.
7. Stefanini GG, Byrne RA, Serruys PW, de Waha A, Meier B, Massberg S, Juni P, Schomig A, Windecker S, Kastrati A. Biodegradable polymer drug-eluting stents reduce the risk of stent thrombosis at 4 years in patients undergoing percutaneous coronary intervention: a pooled analysis of individual patient data from the ISAR-TEST 3, ISAR-TEST 4, and LEADERS randomized trials. Eur Heart J.. 2012;33:1214–22.
8. Han YL, Zhang L, Yang LX, Liu HL, Qu P, Li WM, Jiang TM, Li SM, Jing QM, Zhang QY, Xu B, Li Y, Gao RL. A new generation of biodegradable polymer-coated sirolimus-eluting stents for the treatment of coronary artery disease: final 5-year clinical outcomes from the CREATE study. EuroIntervention. 2012;8:815–22.
9. Wykrzykowska J, Serruys P, Buszman P, Linke A, Ischinger T, Klauss V, Eberli F, Corti R, Wijns W, Morice MC, Di Mario C, Van Geuns RJ, Van Es GA, Juni P, Windecker S. The three year follow-up of the randomised "all-comers" trial of a biodegradable polymer biolimus-eluting stent versus permanent polymer sirolimus-eluting stent (LEADERS). EuroIntervention. 2011;7:789–95.
10. Palepu V, Kiapour A, Goel VK, Moran JM. A unique modular implant system enhances load sharing in anterior cervical interbody fusion: a finite element study. Biomed Eng Online. 2014;13:26
11. Amornvit P, Rokaya D, Keawcharoen K, Thongpulsawasdi N. Stress distribution in implant retained finger prosthesis: a finite element study. J Clin Diagn Res. 2013;7:2851–4.
12. Schwartz RS, Huber KC, Murphy JG, Edwards WD, Camrud AR, Vlietstra RE, Holmes DR. Restenosis and the proportional neointimal response to coronary artery injury: results in a porcine model. J Am Coll Cardiol. 1992;19:267–74.
13. Kornowski R, Hong MK, Tio FO, Bramwell O, Wu H, Leon MB. In-stent restenosis: contributions of inflammatory responses and arterial injury to neointimal hyperplasia. J Am Coll Cardiol. 1998;31:224–30.
14. Schwartz RS, Edelman ER, Carter A, Chronos N, Rogers C, Robinson KA, Waksman R, Weinberger J, Wilensky RL, Jensen DN, Zuckerman BD, Virmani R. Drug-eluting stents in preclinical studies: recommended evaluation from a consensus group. Circulation. 2002;106:1867–73.
15. Chhajed PN, Dickenmann M, Bubendorf L, Mayr M, Steiger J, Tamm M. Patterns of pulmonary complications associated with sirolimus. Respiration. 2006;73:367–74.
16. Morelon E, Stern M, Israel-Biet D, Correas JM, Danel C, Mamzer-Bruneel MF, Peraldi MN, Kreis H. Characteristics of sirolimus-associated interstitial pneumonitis in renal transplant patients. Transplantation. 2001;72:787–90.
17. Sousa JE, Costa MA, Abizaid AC, Rensing BJ, Abizaid AS, Tanajura LF, Kozuma K, Van Langenhove G, Sousa AG, Falotico R, Jaeger J, Popma JJ, Serruys PW. Sustained suppression of neointimal proliferation by sirolimus-eluting stents: one-year angiographic and intravascular ultrasound follow-up. Circulation. 2001;104:2007–11.
18. McFadden EP, Stabile E, Regar E, Cheneau E, Ong AT, Kinnaird T, Suddath WO, Weissman NJ, Torguson R, Kent KM, Pichard AD, Satler LF, Waksman R, Serruys PW. Late thrombosis in drug-eluting coronary stents after discontinuation of antiplatelet therapy. Lancet. 2004;364:1519–21.
19. Kotani J, Awata M, Nanto S, Uematsu M, Oshima F, Minamiguchi H, Mintz GS, Nagata S. Incomplete neointimal coverage of sirolimus-eluting stents: angioscopic findings. J Am Coll Cardiol. 2006;47:2108–11.
20. Katoh H, Shite J, Shinke T, Matsumoto D, Tanino Y, Ogasawara D, Sawada T, Miyoshi N, Kawamori H, Yoshino N, Hirata K. Delayed neointimalization on sirolimus-eluting stents: 6-month and 12-month follow up by optical coherence tomography. Circ J. 2009;73:1033–7.
21. Nakazawa G, Finn AV, Vorpahl M, Ladich ER, Kolodgie FD, Virmani R. Coronary responses and differential mechanisms of late stent thrombosis attributed to first-generation sirolimus- and paclitaxel-eluting stents. J Am Coll Cardiol. 2011;57:390–8.
22. Nebeker JR, Virmani R, Bennett CL, Hoffman JM, Samore MH, Alvarez J, Davidson CJ, McKoy JM, Raisch DW, Whisenant BK, Yarnold PR, Belknap SM, West DP, Gage JE, Morse RE, Gligoric G, Davidson L, Feldman MD. Hypersensitivity cases associated with drug-eluting coronary stents: a review of available cases from the research on adverse drug events and reports (RADAR) project. J Am Coll Cardiol. 2006;47:175–81.
23. Luscher TF, Steffel J, Eberli FR, Joner M, Nakazawa G, Tanner FC, Virmani R. Drug-eluting stent and coronary thrombosis: biological mechanisms and clinical implications. Circulation. 2007;115:1051–8.
24. Windecker S, Serruys PW, Wandel S, Buszman P, Trznadel S, Linke A, Lenk K, Ischinger T, Klauss V, Eberli F, Corti R, Wijns W, Morice MC, di Mario C, Davies S, van Geuns RJ, Eerdmans P, van Es GA, Meier B, Juni P. Biolimus-eluting stent with biodegradable polymer versus sirolimus-eluting stent with durable polymer for coronary revascularisation (LEADERS): a randomised non-inferiority trial. Lancet. 2008;372:1163–73.
25. Serruys PW, Farooq V, Kalesan B, de Vries T, Buszman P, Linke A, Ischinger T, Klauss V, Eberli F, Wijns W, Morice MC, Di Mario C, Corti R, Antoni D, Sohn HY, Eerdmans P, Rademaker-Havinga T, van Es GA, Meier B, Juni P, Windecker S. Improved safety and reduction in stent thrombosis associated with biodegradable polymer-based biolimus-eluting stents versus durable polymer-based sirolimus-eluting stents in patients with coronary artery disease: final 5-year report of the LEADERS (Limus Eluted From A Durable Versus ERodable Stent Coating) randomized, noninferiority trial. JACC Cardiovasc Interv. 2013;6:777–89.
26. Smits PC, Hofma S, Togni M, Vazquez N, Valdes M, Voudris V, Slagboom T, Goy JJ, Vuillomenet A, Serra A, Nouche RT, den Heijer P, van der Ent M. Abluminal biodegradable polymer biolimus-eluting stent versus durable polymer everolimus-eluting stent (COMPARE II): a randomised, controlled, non-inferiority trial. Lancet. 2013;381:651–60.
27. Lupi A, Gabrio Secco G, Rognoni A, Lazzero M, Fattori R, Sheiban I, Sante Bongo A, Bolognese L, Agostoni P, Porto I. Meta-analysis of bioabsorbable versus durable polymer drug-eluting stents in 20,005 patients with coronary artery disease: an update. Catheter Cardiovasc Interv. 2014;83:E193–206.
28. Hagiwara H, Hiraishi Y, Terao H, Hirai T, Sakaoka A, Sasaki M, Murota S, Inoue K, Kimura J. Vascular responses to a biodegradable polymer (polylactic acid) based biolimus A9-eluting stent in porcine models. EuroIntervention. 2012;8:743–51.
29. Wiebe J, Nef HM, Hamm CW. Current status of bioresorbable scaffolds in the treatment of coronary artery disease. J Am Coll Cardiol. 2014;64:2541–51.
30. Verheye S, Ormiston JA, Stewart J, Webster M, Sanidas E, Costa R, Costa JR Jr., Chamie D, Abizaid AS, Pinto I, Morrison L, Toyloy S, Bhat V, Yan J, Abizaid A. A next-generation bioresorbable coronary scaffold system: from bench to first clinical evaluation: 6- and 12-month clinical and multimodality imaging results. JACC Cardiovasc Interv. 2014;7:89–99.
31. Rogers CD. Optimal stent design for drug delivery. Rev Cardiovasc Med. 2004;5(Suppl 2):S9–S15.
32. Basalus MW, van Houwelingen KG, Ankone M, de Man FH, von Birgelen C. Scanning electron microscopic assessment of the biodegradable coating on expanded biolimus-eluting stents. EuroIntervention. 2009;5:505–10.